

Supporting Information

PcxL and HpxL are flavin-dependent, oxime-forming *N*-oxidases in phosphonocystoximic acid biosynthesis in *Streptomyces*

Michelle N. Goettge, Joel P. Cioni, Kou-San Ju, Katharina Pallitsch, William W. Metcalf

Table S1: Putative phosphonocystoximate and hydroxyphosphonocystoximate gene clusters	S-2
Figure S1: Putative phosphonocystoximate and hydroxyphosphonocystoximate gene clusters.....	S-3
Figure S2: Characterization of HpxL and PcxL as FAD-dependent enzymes.....	S-4
Figure S3: ^1H - ^{31}P HMBC NMR analysis of HpxL using 2AEPn as substrate.....	S-5
Figure S4: ^1H - ^{31}P HMBC NMR analysis of PcxL using 2AEPn as substrate.....	S-6
Figure S5: ^1H - ^{31}P HMBC NMR analysis of HpxL using (<i>S</i>)-1H2AEPn as substrate.....	S-7
Figure S6: ^1H - ^{31}P HMBC NMR analysis of PcxL using (<i>S</i>)-1H2AEPn as substrate.....	S-8

Table S1. Comparison of the phosphonocystoximate (Pcx) and hydroxyphosphonocystoximate (Hpx) gene clusters. Genes with the same corresponding fourth letter of the gene are homologous to one another. Percent amino acid identity between the proteins is given based on BLAST. NP = not present within the gene cluster and N/A= not applicable

Pcx Gene	Size (#AA)	Accession Number	Hpx Gene	Size (#AA)	Accession Number	%Identity	Putative Function / Description	Pfam
<i>pcxA</i>	404	WP_030230281.1	<i>hpxA</i>	409	WP_030990657.1	57%	Helix-turn-helix domain transcriptional regulator	PF13560
<i>pcxB</i>	60	WP_030230290.1	<i>hpxB</i>	201	WP_030646389.1		Hypothetical protein	No Match
<i>pcxC</i>	412	WP_051704820.1	<i>hpxC</i>	414	WP_030990660.1	64%	ATP-grasp domain containing protein	PF13535
<i>pcxD</i>	413	WP_051704821.1	<i>hpxD</i>	415	WP_048910652.1	70%	ATP-grasp domain containing protein	PF13535
<i>pcxE</i>	484	WP_030230301.1	<i>hpxE</i>	456	WP_030990665.1	58%	Condensation domain containing protein	PF00668
<i>pcxF</i>	426	WP_051704822.1	<i>hpxF</i>	422	WP_048910653.1	76%	Biotin carboxylase / ATP-grasp domain	PF13535
<i>pcxG</i>	418	WP_030230306.1	<i>hpxG</i>	419	WP_030990668.1	70%	Major facilitator superfamily transporter	PF07690
<i>pcxH</i>	434	WP_030230310.1	<i>hpxH</i>	447	WP_030646400.1	63%	Peptidase	PF01523
<i>pcxI</i>	451	WP_051704823.1	<i>hpxI</i>	447	WP_048910654.1	77%	Peptidase	PF01523
<i>pcxJ</i>	213	WP_030230320.1	NP	N/A	N/A	N/A	Pyridoxamine 5'-phosphate oxidase	PF10590
<i>pcxK</i>	237	WP_030230324.1	<i>hpxK</i>	241	WP_030646417.1	58%	Mycothiol-dependent maleylpyruvate isomerase	PF11716
<i>pcxL</i>	742	WP_051704824.1	<i>hpxL</i>	750	WP_030990682.1	61%	NAD_binding_9 FAD-NAD(P)-binding	PF13454
<i>pcxM</i>	363	WP_037834389.1	<i>hpxM</i>	375	WP_030990679.1	66%	Aminotransferase class-V	PF00266
<i>pcxN</i>	307	WP_030230335.1	<i>hpxN</i>	290	WP_030990678.1	55%	Fosfomycin resistance kinase FomA	PF00696
<i>pcxO</i>	215	WP_030230340.1	NP	N/A	N/A	N/A	Thymidylate kinase	PF02223
<i>pcxP</i>	90	WP_030230342.1	NP	N/A	N/A	N/A	Phosphopantetheine-binding protein	PF00550
<i>pcxQ</i>	371	WP_037834390.1	<i>hpxQ</i>	395	WP_030990677.1	66%	Uncharacterized nucleotidyltransferase	PF14907
<i>pcxR</i>	549	WP_030230346.1	<i>hpxR</i>	563	WP_030990676.1	58%	Non-ribosomal peptide synthetase adenylation domain	PF00501
<i>pcxS</i>	353	WP_030230349.1	<i>hpxS</i>	349	WP_030990674.1	72%	2,3-diaminopropionate biosynthesis protein SbnB	PF02423
<i>pcxT</i>	322	WP_037834298.1	<i>hpxT</i>	324	WP_030646404.1	67%	2,3-diaminopropionate biosynthesis protein SbnA	PF00291
<i>pcxU</i>	286	WP_030230355.1	<i>hpxU</i>	286	WP_030646403.1	72%	Phosphoenolpyruvate phosphomutase	PF13714
NP	N/A	N/A	<i>hpxV</i>	322	WP_030990672.1	N/A	TauD taurine catabolism dioxygenase	PF02668
NP	N/A	N/A	<i>hpxW1</i>	167	WP_030646419.1	N/A	Phosphonopyruvate decarboxylase alpha subunit	PF02776
NP	N/A	N/A	<i>hpxW2</i>	182	WP_030646420.1	N/A	Phosphonopyruvate decarboxylase beta subunit	PF02775
NP	N/A	N/A	<i>hpxX</i>	86	WP_030990685.1	N/A	Acyl carrier protein	PF00550
NP	N/A	N/A	<i>hpxY</i>	337	WP_030990687.1	N/A	FomB family phosphonate monophosphate kinase	PF13481
NP	N/A	N/A	<i>hpxZ</i>	284	WP_030646426.1	N/A	EamA-like transporter family protein	PF00892
<i>orf1</i>	316	WP_037834300.1	NP	N/A	N/A	N/A	3-phosphoglycerate dehydrogenase	PF02826
<i>orf2</i>	367	WP_051704838.1	NP	N/A	N/A	N/A	L-iditol 2-dehydrogenase	PF08240
<i>orf3</i>	365	WP_030230374.1	NP	N/A	N/A	N/A	N-acetyl-gamma-glutamyl-phosphate reductase	PF01118
<i>orf4</i>	418	WP_051704825.1	NP	N/A	N/A	N/A	Phosphoglycerate kinase	PF00162
<i>orf5</i>	373	WP_030230380.1	NP	N/A	N/A	N/A	1,3-propanediol dehydrogenase	PF00465
<i>orf6</i>	202	WP_030230383.1	NP	N/A	N/A	N/A	DUF402 containing protein	PF04167

***Streptomyces* sp. NRRL S-481**



***Streptomyces regensis* NRRL WC-3744**

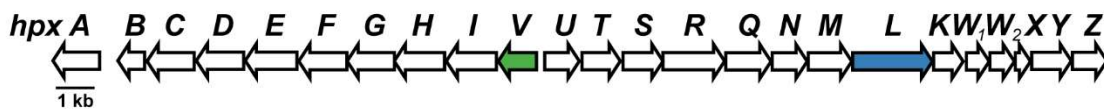


Figure S1. The putative biosynthetic gene clusters for phosphonocystoximate and hydroxyphosphonocystoximate, found in *Streptomyces* sp. NRRL S-481 and *Streptomyces regensis* NRRL WC-3744, respectively. Putative gene functions are shown in Table S1.

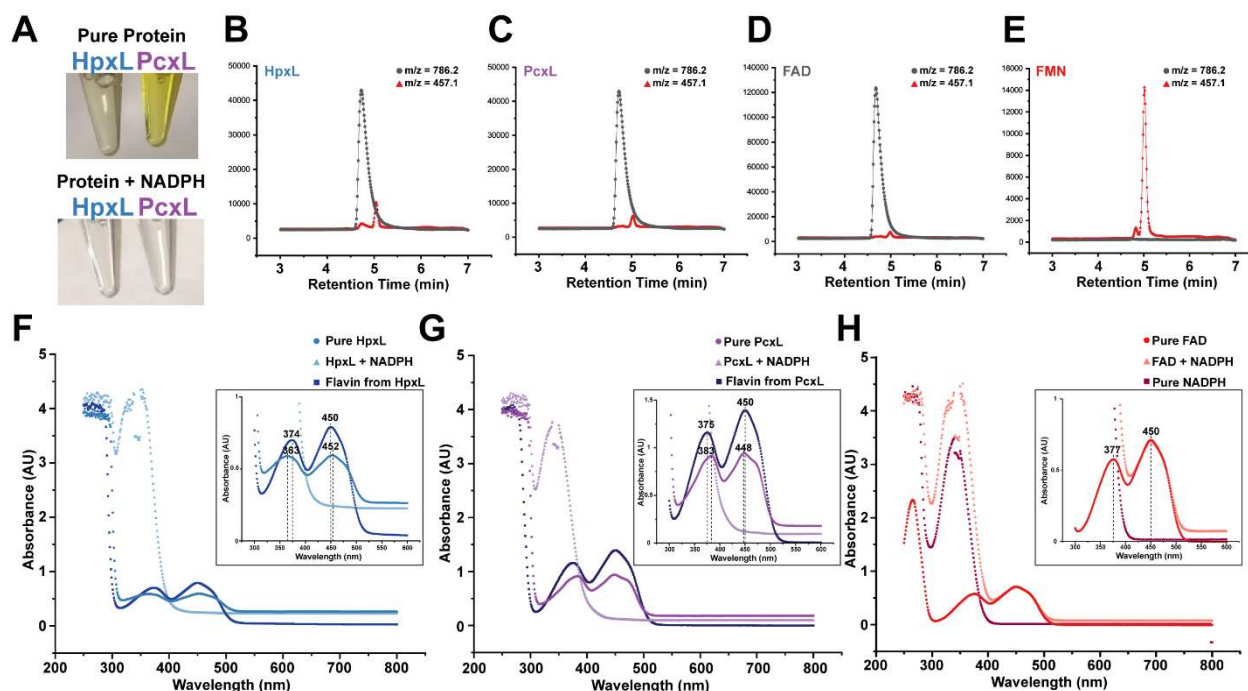


Figure S2. Characterization of HpxL and PcxL as FAD-dependent enzymes. (A) The top photograph is of purified 6xHis tagged *N*-oxidases after purification. The bottom photograph shows the enzyme after incubation with NADPH. (B-E) Low resolution mass spectrometry of the flavin isolated from (B) HpxL (37.1 μ M) and (C) PcxL (30.9 μ M). (D) FAD standards and (E) FMN standards were used at a concentration of 50 μ M. (F) HpxL absorption spectra of purified flavin (dark blue squares) or HpxL before (blue circles) and after (light blue triangles) incubation with NADPH. Inset shows the maximum absorption of HpxL at 363 nm and 452 nm. Purified flavin from washed HpxL shows absorption maxima at 374 nm and 450 nm. (G) PcxL absorption spectra of purified flavin (dark purple squares) or the protein before (purple circles) and after (light purple triangles) incubation with NADPH. Inset shows the maximum absorption of PcxL at 383 nm and 448 nm. Purified flavin from washed PcxL shows absorption maxima at 377 nm and 450 nm. (H) Control reactions showing FAD absorption (red circles), NADPH absorption (dark red squares), and a mixture of pure FAD and NADPH (pink triangles). The inset shows the absorption maxima of FAD at 377 nm and 450 nm. The elevated baseline in the spectra shown in (F) and (G) are likely due to light scattering from small amounts of protein precipitation of HpxL and PcxL, as baseline elevation is not observed with the purified flavin that was washed from the proteins. We have observed that HpxL and PcxL are not stable for an extended period of time in solution at room temperature.

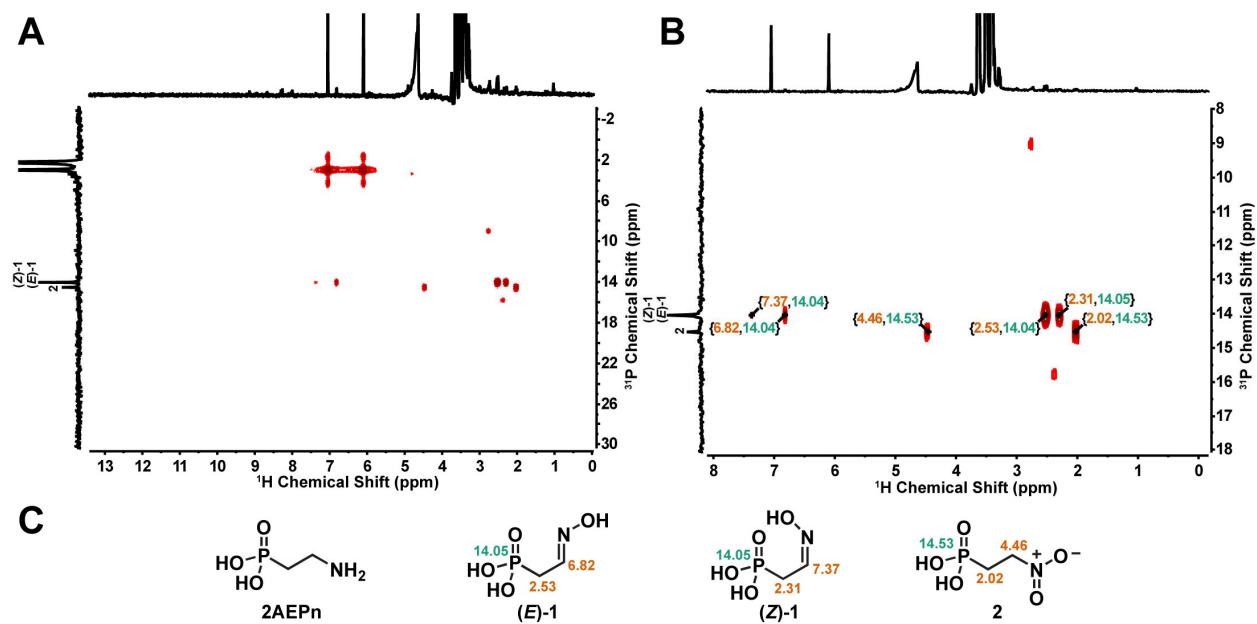


Figure S3. HMBC NMR analysis of HpxL incubated in the presence of FAD, NADPH, and 2AEPn for 16 hours. (A) ^1H - ^{31}P HMBC spectrum of the HpxL reaction with 2AEPn as the substrate showing all phosphorus-containing molecules in the reaction. (B) Magnified region of the ^1H - ^{31}P spectrum with key proton-phosphorus correlations labeled (^1H chemical shift, ^{31}P chemical shift). (C) Compounds identified using ^1H - ^{31}P correlations with the ^1H chemical shifts displayed in orange and ^{31}P chemical shift in green. 2AEPn, (*E*)- and (*Z*)-**1**, and **2** are shown. Substrates and cofactors were added at the following concentrations: 100 μM FAD, 500 μM NADPH, 3 mM 2AEPn, and 25 μM HpxL. 25 mM phosphite and 10 μM PTDH17x were also included as a cofactor regenerating system.

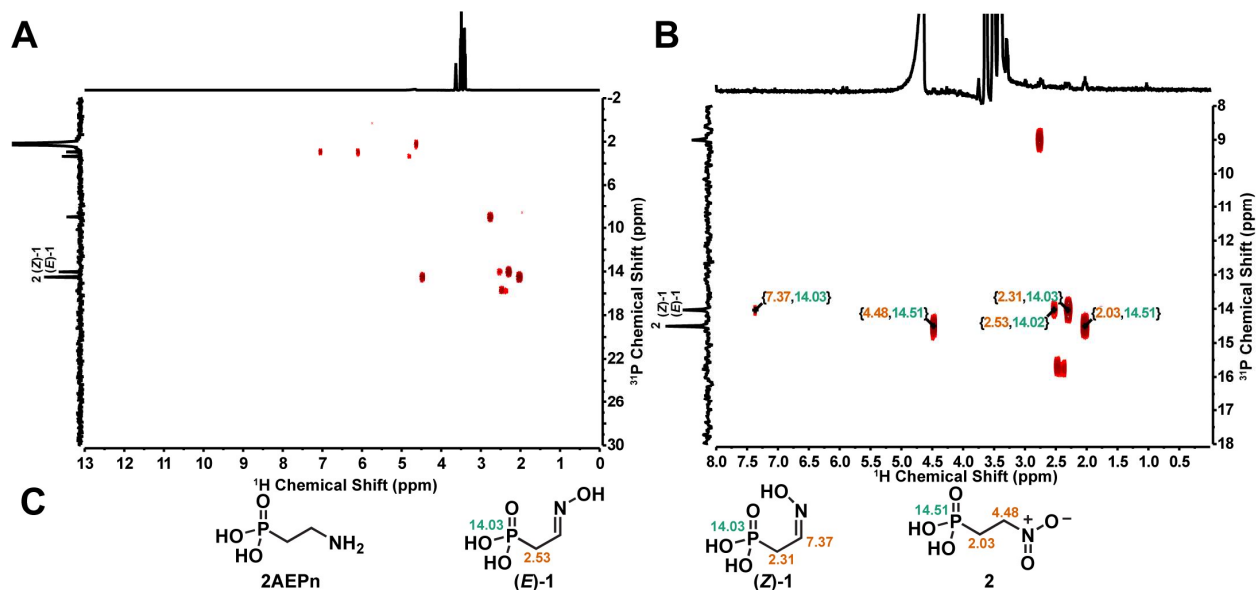


Figure S4. HMBC NMR analysis of PcxL incubated in the presence of FAD, NADPH, and 2AEPn for 16 hours. (A) ^1H - ^{31}P HMBC NMR spectra of the PcxL reaction with 2AEPn as the substrate showing all phosphorus-containing molecules in the reaction. (B) Magnified region of the ^1H - ^{31}P spectrum with key proton-phosphorus correlations labeled (^1H chemical shift, ^{31}P chemical shift). (C) Compounds identified using ^1H - ^{31}P correlations with the ^1H chemical shifts displayed in orange and ^{31}P chemical shift in green. 2AEPn, (E)- and (Z)-1 and 2 are shown. Substrates and cofactors were added at the following concentrations: 100 μM FAD, 500 μM NADPH, 3 mM 2AEPn, and 25 μM PcxL. 25 mM phosphite and 10 μM PTDH17x were also added as a cofactor regenerating system.

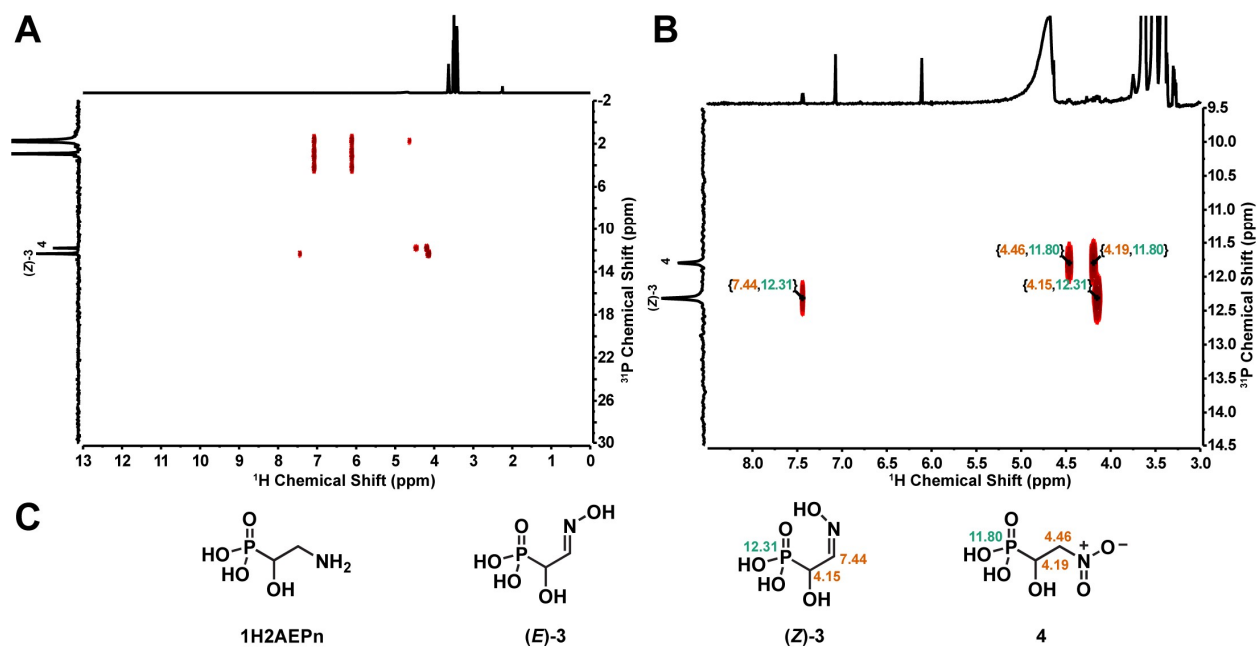


Figure S5. HMBC NMR analysis of HpxL incubated in the presence of FAD, NADPH, and (*S*)-1H2AEPn for 16 hours. (A) ¹H-³¹P HMBC NMR spectra of the HpxL reaction with (*S*)-1H2AEPn as the substrate showing all phosphorus-containing molecules in the reaction. (B) Magnified region of the ¹H-³¹P spectrum with key proton-phosphorus correlations labeled (¹H chemical shift, ³¹P chemical shift}). (C) Compounds identified using ¹H-³¹P correlations with the ¹H chemical shifts displayed in orange and ³¹P chemical shift in green. 1H2AEPn, (*E*)- and (*Z*)-**3** and **4** are shown. Substrates and cofactors were added at the following concentrations: 100 μM FAD, 500 μM NADPH, 3 mM (*S*)-1H2AEPn, and 25 μM HpxL. 25 mM phosphite and 10 μM PTDH17x were also as a cofactor regenerating system.

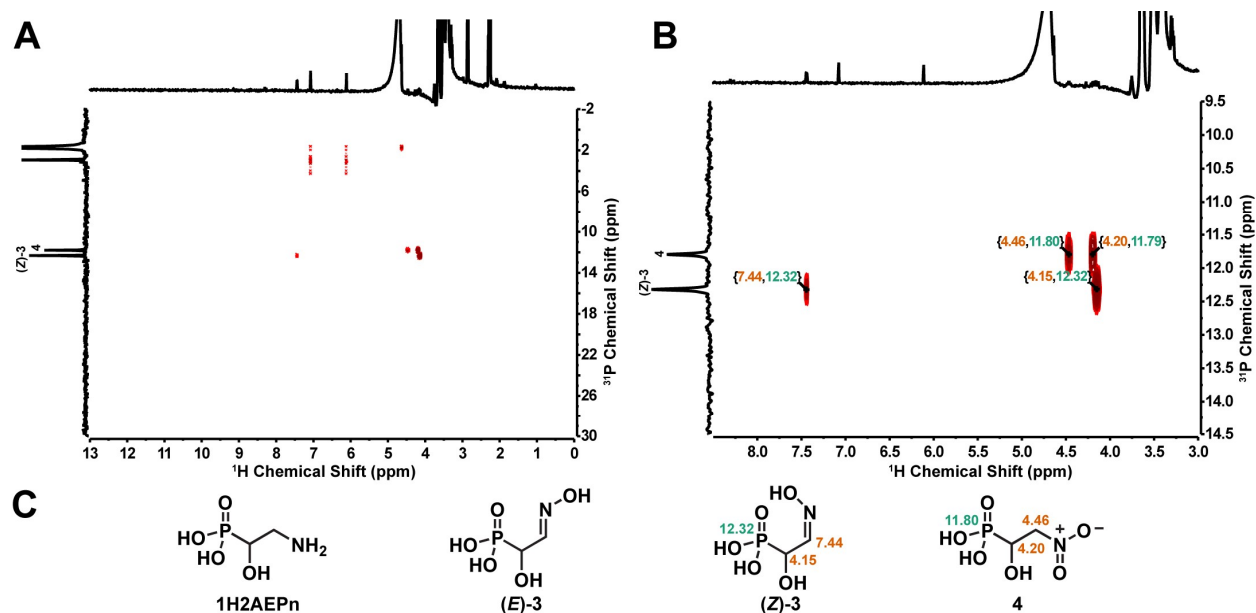


Figure S6. PcxL was incubated in the presence of FAD, NADPH, and (*S*)-1H2AEPn for 16 hours. (A) ^1H - ^{31}P HMBC NMR spectra of the HpxL reaction with (*S*)-1H2AEPn as the substrate showing all phosphorus-containing molecules in the reaction. (B) Magnified region of the ^1H - ^{31}P spectrum with key proton-phosphorus correlations labeled ($\{^1\text{H}$ chemical shift, ^{31}P chemical shift $\}$). (C) Compounds identified using ^1H - ^{31}P correlations with the ^1H chemical shifts displayed in orange and ^{31}P chemical shift in green. (*S*)-1H2AEPn, (*E*)- and (*Z*)-**3** and **4** are shown. Substrates and cofactors were added at the following concentrations: 100 μM FAD, 500 μM NADPH, 3 mM (*S*)-1H2AEPn, and 25 μM PcxL. 25 mM phosphite and 10 μM PTDH17x were also as a cofactor regenerating system.